



www.sciencemag.org/cgi/content/full/316/5827/1014/DC1

Supporting Online Material for

Molecular Basis of the Shish-Kebab Morphology in Polymer Crystallization

Shuichi Kimata, Takashi Sakurai, Yoshinobu Nozue,* Tatsuya Kasahara, Noboru Yamaguchi, Takeshi Karino, Mitsuhiro Shibayama, Julia A. Kornfield*

*To whom correspondence should be addressed.

E-mail: nozue@sc.sumitomo-chem.co.jp (Y.N.); jak@caltech.edu (J.A.K.)

Published 18 May, *Science* **316**, 1014 (2007)

DOI: 10.1126/science.1140132

This PDF file includes:

Materials and Methods

SOM Text

Figs. S1 to S7

Tables S1 and S2

References

SUPPORTING MATERIAL**Materials**

Hydrogenated and deuterated isotactic polypropylene (H-iPP and D-iPP) were polymerized with propene (C_3H_6) and deuterated propene (C_3D_6) respectively by an isospecific metallocene catalyst system; dimethylsilyl bis(2-methyl-4-naphthylindenyl) zirconium dichloride and methyl aluminoxane in toluene. In order to control the molecular weight of hydrogenated and deuterated iPP, polymerization temperature was controlled. Using selected reaction temperatures between 15°C to 70°C, six different molecular weights of H-iPP and three different molecular weights of D-iPP were prepared. Using high-temperature GPC with *o*-dichlorobenzene as an eluent and calibration based on polystyrene standards, molecular weight (M_w) and polydispersity (M_w/M_n) was measured for each of these H-iPPs and D-iPPs (Table S1).

Table S1. Molecular weight (M_w) and polydispersity (M_w/M_n) of H-iPPs and D-iPPs

Sample Name	Isotope Labeling	M_w	M_w/M_n
H-s	H	49,200	2.3
H-m1		185,800	3.3
H-m2		234,400	3.4
H-m3		242,500	3.2
H-l1		996,300	2.6
H-l2		1,419,900	2.8
D-s	D	40,900	2.4
D-m		196,700	3.2
D-l		1,780,900	3.1

To understand the behavior of broad distribution iPPs that have enormous technological relevance and have been widely studied, we designed blends of the above

components to produce polydispersity of $M_w/M_n \approx 8$. Based on the measured molar mass distributions, we computed the amount of each species such that each blend would each have M_w 490,000 g/mol and 13.3% of deuterium-labelled chains (Table S2). To ensure uniform molecular dispersion of the components, the three model iPP resins with deuterium labeling (Short-D, Medium-D and Long-D) were prepared by solution blending: the specified masses of the H-iPP and D-iPP species were dissolved in boiling xylene (350 mL) in the presence of antioxidant (1000ppm of IRGANOX1010 and 2000ppm of IRGAFOS168, distributed by Ciba Specialty Chemicals) and then precipitated into methanol with vigorous stirring. The resulting blends were dried at 60°C in vacuum.

Table S2. Blend compositions of the deuterium-labeled model iPP resins

Model iPP	H-iPP (g)						D-iPP (g)		
	H-s	H-m1	H-m2	H-m3	H-I1	H-I2	D-s	D-m	D-I
Short-D	-	1.5	1.5	1.5	1.0	1.0	1.0	-	-
Medium-D	1.0	0.5	1.5	1.5	1.0	1.0	-	1.0	-
Long-D	1.0	1.5	1.5	1.5	0.5	0.5	-	-	1.0

A variety of measurements were used to confirm that the three model resins were adequately well matched: high-temperature GPC measurement of their molar mass distribution and rheo-optical characterization of their behavior during flow and subsequent crystallization. The rheo-optical measurements provided the basis for selecting the conditions for inducing highly oriented crystallization.

Shear-induced crystallization of deuterium labeled iPP resins

Pressure driven flow through a rectangular slit was used to impose a well-defined flow and thermal history. A custom apparatus subjects the sample to a specified, high wall shear stresses for a controlled duration, continuously monitoring the birefringence and turbidity of the sample during and after shear (*SI*). Rheo-optical studies guided the

selection of shearing temperature ($T_s=180^\circ\text{C}$) and crystallization temperature ($T_c=140^\circ\text{C}$), and established that a shear stress of 0.14MPa was high enough to induce the transition to highly oriented crystallization (S2). The flow-cell was initially held at 215°C and filled with polymer melt from the reservoir. The polymer in the flow-cell was then held at 215°C for 10 min to erase any memory effects caused by the filling process. The sample was cooled to $T_s=180^\circ\text{C}$ and allowed to reach a uniform temperature. Control samples (unsheared) and oriented samples (sheared as follows) were prepared for each of the three blends. For the oriented samples, once the temperature equilibrated at 180°C , a pressure drop across the length of the channel was applied to drive shear flow through the channel at a wall shear stress of 0.14MPa for a brief shearing time (1.0sec). Immediately after imposing short-term shearing (or none for the control), the flow-cell was cooled to 140°C (cooling at approximately $4^\circ\text{C}/\text{min}$) and then held

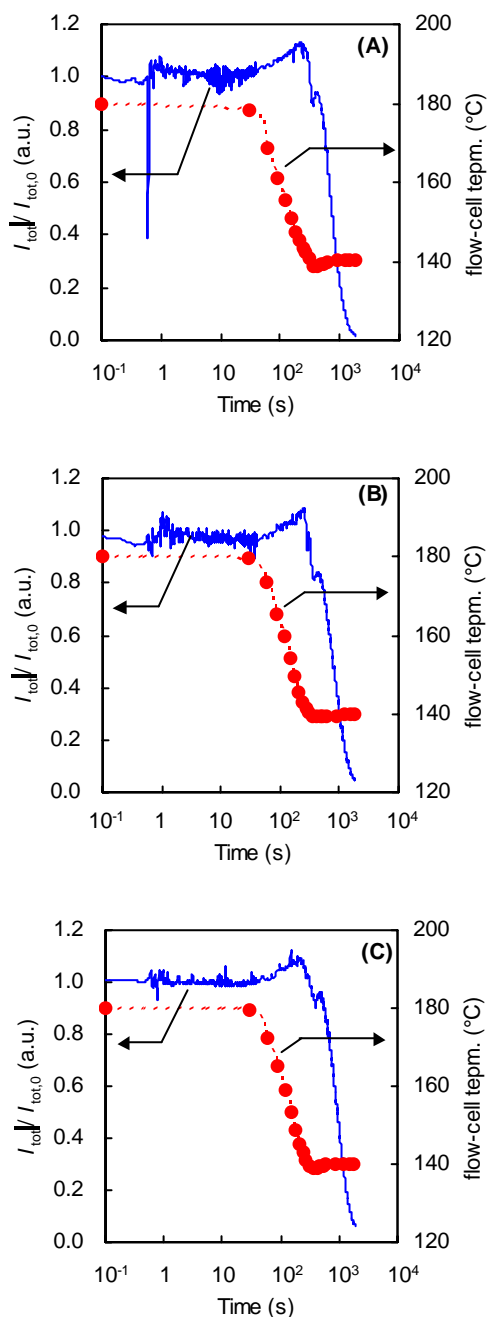


Figure S1. Turbidity and flow-cell temperature of (A) Short-D, (B) Medium-D and (C) Long-D during and after short-term shearing. The temperature during cooling from the shearing temperature (180°C) to the crystallization temperature (140°C) is shown for reference.

at 140°C for 20min. The turbidity and birefringence were tracked to monitor the progress and anisotropy of crystallization of model iPP resins. After 20 minutes, to complete solidification of the sample, the flow-cell was removed from the apparatus and plunged in cold water.

The optical train used for the measurements was the same as described previously (S3). The intensity of He-Ne laser light passing through crossed and parallel polarizers (I_{\perp} and I_{\parallel}) was measured with photodiode detectors. When depolarization is negligible, the birefringence (Δn), which is a measure of the mean anisotropy of the sample, is given by

$$\Delta n = \frac{\lambda}{\pi d} \sin^{-1} \left(\sqrt{\frac{I_{\perp}}{I_{\perp} + I_{\parallel}}} \right)$$

where λ is the wavelength of light (632.8nm) and d is the thickness of the sample. Transmittance is defined as total transmitted intensity ($I_{\text{tot}} = I_{\perp} + I_{\parallel}$) normalized by a constant value of $I_{\text{tot},0}$ before shearing.

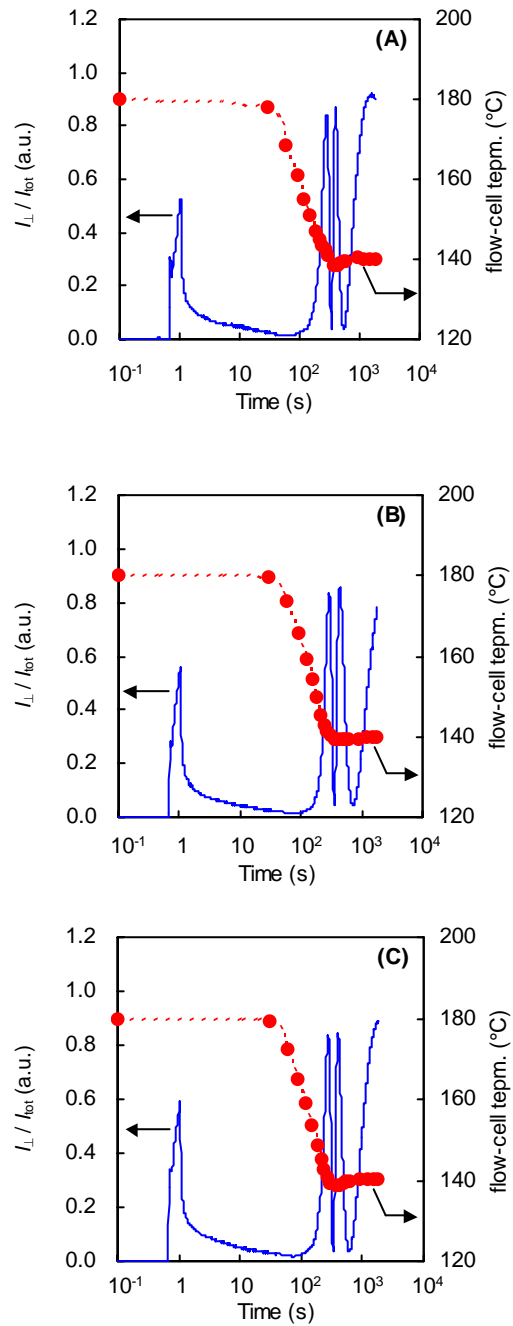


Figure S2. Relative intensity through crossed polarizers (I_{\perp}/I_{tot}) and flow-cell temperature of (A) Short-D, (B) Medium-D and (C) Long-D during and after short-term shearing, recorded simultaneously with the transmitted intensity in Figure S1.

For the quiescently crystallized samples, the transmittance traces are very similar for the three materials (not shown). During shear-induced crystallization the transient transmittance (Figure S1) and retardance (Figure S2) are very similar for all three resins. As for the transmittance trace, formation of scatterers becomes evident when the temperature reaches approximately 150°C (manifested by the drop in transmittance), there is a brief local minimum approximately 100s later, and the transmitted intensity falls to approximately 20% at 1,000s. In situ measurements end at 1,200s when the flow cell is removed from the apparatus and plunged into cold water.

Upon inception of shear the retardance passes through the usual overshoot characteristic of highly entangled melts of high polydispersity (Figure S2). The subsequent increase in birefringence between $t=0.5$ s and the conclusion of shearing at 1s is characteristic of highly oriented crystallization and it is almost identical for all three samples. Upon cessation of shear the retardance drops rapidly, evident in the drop to $I_{\perp}/I_{\text{tot}} = 0.1$ for all samples; thus, the blends were very well matched in terms of the extent of oriented crystallization during flow. Subsequently, while held at 180°C, the retardance slowly decreased in the same way for all samples. During cooling from 180°C to 140°C, the retardance began to rise again, indicative of growth of oriented crystallites, at $t \approx 200$ s when $T \approx 150^{\circ}\text{C}$. The retardance ($2\pi d\Delta n/\lambda$) passed over orders with successive maxima in I_{\perp}/I_{tot} corresponding to increasing, odd multiples of 1/2 and successive minima correspond to even multiples of 1/2. The excellent match of the times to reach each order (e.g., retardance reaches 2 waves at $t=800$ s for all three samples) is a very strong indication that the density of shish created during flow and the growth of kebabs on them are virtually identical in all samples. At 1,800s the transmittance was 5%, each optical experiment was terminated and the sample was rapidly cooled to ambient temperature, as above.

Ex-situ examination of the morphology of the samples using optical microscopy with polarized light (Figure S3), transmission electron microscopy (Figure S4), wide-angle x-ray scattering (Figure S5 and S6) and small-angle x-ray scattering (Figure S7) confirmed that their structure on length scales from 100 μm down to <1nm was well matched. The oriented skin is very uniform in thickness (dark layers near the surface when viewed with

polarizer along the flow direction and analyzer orthogonal to it, Figure S3) and uniform in nanostructure (Figure S4). The spherulitic structure in the core of the sample has a very fine length scale, indicative of crystallization at temperatures below 100°C: negligible crystallization in this zone occurred during the 20 minutes prior to rapid cooling from 140°C to ambient temperature.

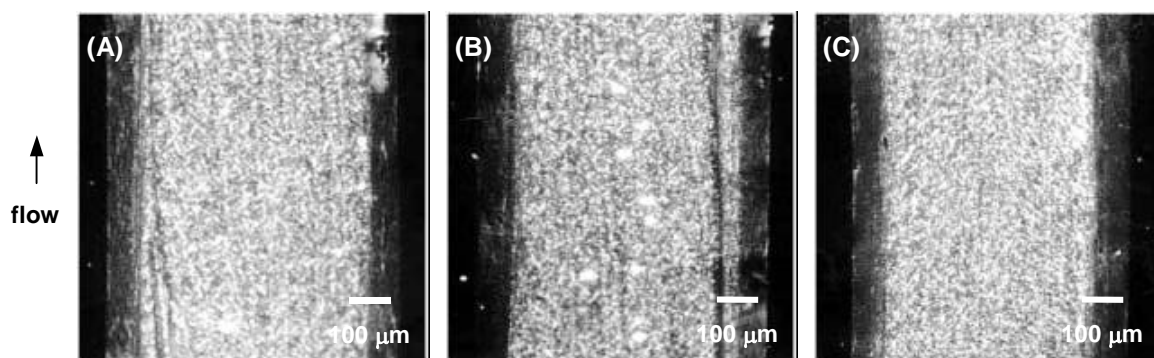


Figure S3. Polarized optical micrograph of cross section of solidified specimen ((A) Short-D, (B) Medium-D and (C) Long-D). Relative to the flow direction, the polarizer and analyzer are oriented parallel and orthogonal, respectively.

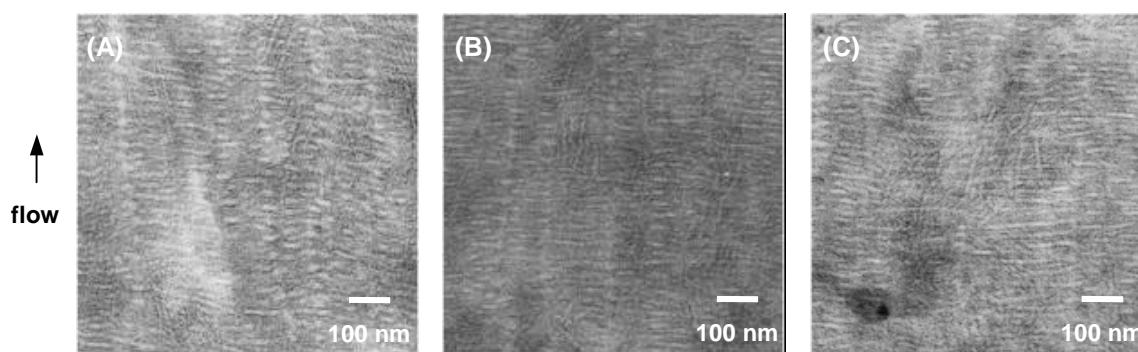


Figure S4. Transmittance electron micrograph of skin layer of solidified specimen ((A) Short-D, (B) Medium-D and (C) Long-D).

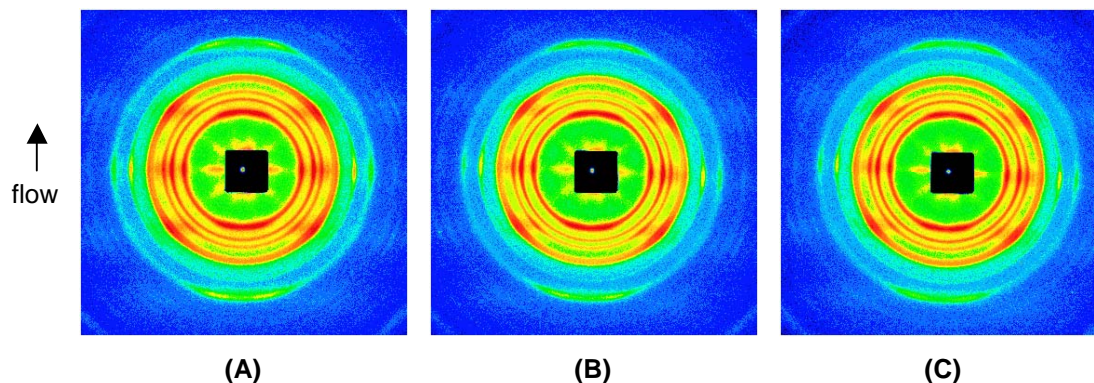


Figure S5. Two-dimensional WAXS pattern of solidified specimen of (A) Short-D, (B) Medium-D and (C) Long-D.

Small angle neutron scattering (SANS) measurements

SANS measurements were performed on the SANS-U instrument owned by the Institute for Solid-State Physics of the University of Tokyo, at the research reactor JRR-3 located at the Japan Atomic Energy Research Institute, Tokai Japan (S4). A flux of cold neutrons with wavelength $\lambda = 7.0\text{\AA}$ was incident on the sample, and the scattered intensity profiles were collected with an area detector of

$128 \text{ pixels} \times 128 \text{ pixels}$. The sample-to-detector distances were set to 2m and 8m, which covered an accessible q range of $0.006\text{--}0.1 \text{ \AA}^{-1}$. Here, q is the scattering vector defined as $4\pi \sin\theta/\lambda$ and 2θ is the scattering angle. Scattered intensities were corrected for cell

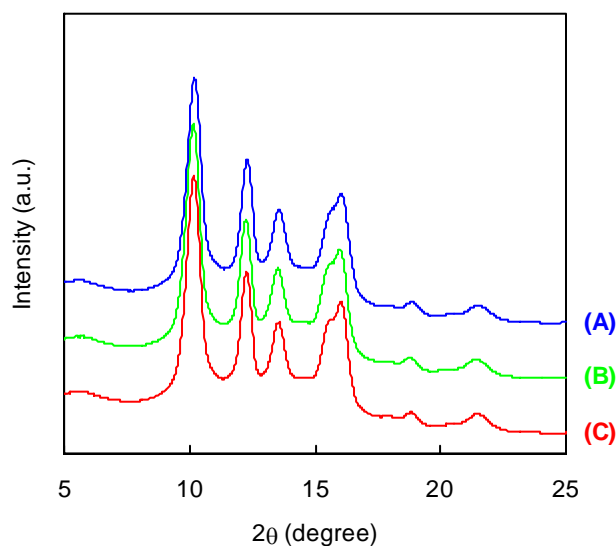


Figure S6. Circularly averaged WAXS pattern of solidified specimen of (A) Short-D, (B) Medium-D and (C) Long-D

scattering, transmission, and incoherent scattering, and then scaled to the absolute intensities with a polyethylene standard sample (Lupolen) (S4, S5). All samples were placed under vacuum to avoid degradation when heated from 25°C to 180°C at 2°C/min.

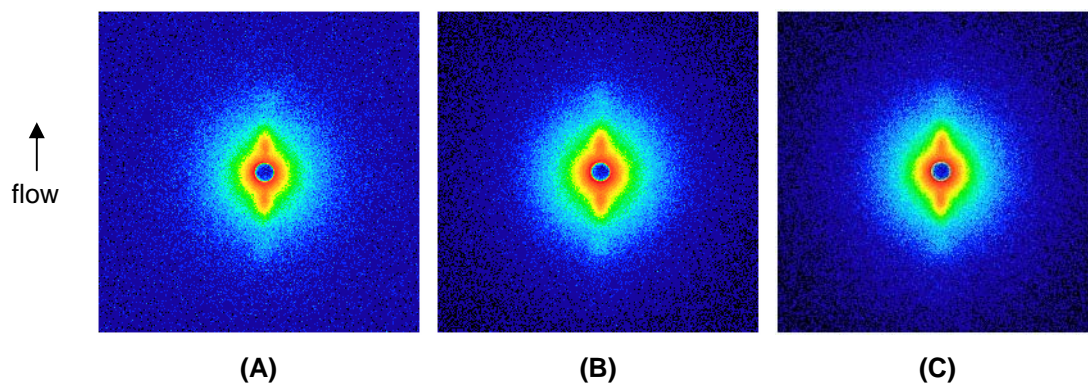


Figure S7. Two-dimensional SAXS pattern of solidified specimens of (A) Short-D, (B) Medium-D and (C) Long-D.

References

- S1. G. Kumaraswamy, R. K. Verma, J. A. Kornfield, *Rev. Sci. Inst.*, **70**, 2097 (1999)
- S2. G. Kumaraswamy, J. A. Kornfield, F. Yeh, B. S. Hsiao, *Macromolecules* **35**, 1762 (2002)
- S3. G. Kumaraswamy, A. M. Issaian, J. A. Kornfield, *Macromolecules* **32**, 7537 (1999)
- S4. S. Okabe, et al., *J. Appl. Crystallography*, **38**, 1035, (2005)
- S5. M. Shibayama, M. Nagao, S. Okabe, T. Karino, *J. Phys. Soc. Jpn.* **74**, 2728 (2005)